IJE TRANSACTIONS A: Basics Vol. 27, No. 1, (January 2014) 143-156

International Journal of Engineering

Journal Homepage: www.ije.ir

Design, Construction and Comparison of a Sensorless Driver Circuit for Switched Reluctance Motor

M. Rafiee * [a], E. Afjei[b], A. Siadatan[a]

[a] *Department of Electrical Engineering, West Tehran Branch, Islamic Azad University, Tehran, Iran*
[b] *Department of Electrical Engineering, Faculty of Electrical and Computer Engineering, Shahid Beheshti University, Tehran, Iran*

PAPER INFO

Paper history:
Received 27 March 2013
Received in revised form 27 April 2013
Accepted 20 June 2013

Keywords:
Sensorless
SRM
FEM

ABSTRACT

In the presented paper, a sensorless driver circuit is designed, constructed and tested to control two types of three-phase Switched Reluctance Motor (SRM). The presented control algorithm has three steps. In the first step, the SRM is started and controlled by an open-loop method. In the second step, a novel method is introduced which uses the optimized flux-current-rotor position relation in order to calculate the position of the rotor and then control the motor in low speed. In the third step, the current waveform of the excited phase of the motor is utilized in order to detect the rotor position and control the SRM in high speed. Because of using the presented novel method, a low cost and simple sensorless driver circuit has been designed. In the circuit, an inexpensive Atmega128 AVR microcontroller is used to implement the control algorithms and generate gate pulses of transistors. Asymmetric bridge converter with N-channel Mosfets is used in order to excite the winding of phases. The parameters of the SRMs which are required for designing the sensorless driver circuit are obtained by simulating and analyzing the motors by Finite Element Method (FEM). The constructed circuit is tested in laboratory by driving the selected SRMs in no-load condition and the operational results are obtained and compared to each other at the end.

doi: *10.5829/idosi.ije.2014.27.01a.17*

1. INTRODUCTION

The SRM driver uses some power electronic devices and transistors; as a result, it had not been a favorable motor for many years till improvement in power electronic in last decades. SRM controlling requires the rotor position information. The stator phase should be excited in a position of the rotor at which positive torque is generated and the rotor rotates. In general, two methods are used in SRM control: direct and indirect (sensorless) strategies. [1, 2]

In direct strategies, position sensors are used to detect the rotor position. Use of position sensors in motor construction offers some disadvantages like less efficiency, less reliability, more wiring, increasing the cost, etc, so sensorless strategies are preferred often.

Some sensorless techniques are explained below. These techniques are classified on their operational speed according to Figure 1.

*Corresponding Author Email: rafiee.mehran@ieee.org (M. Rafiee)

1. **Lock Rotor Strategy:**
   In this method, one phase of the SRM is turned on. The rotor may be aligned with the phase pole. After alignment the rotor position is known and using an affordable switching algorithm, it can rotate. The rotor may rotate a little backward in this technique [3].
2. **Training Pulse Strategy**
   In training pulse technique, trains of pulse are applied to each phase one by one. The rotor will follow the pulses and starts rotating. In this method, the rotor may move reverse some degrees at the first [4].
3. **Pulse Detection Technique**
   Low level high frequency pulses are applied to each phase winding in this technique. The behavior of phases illustrates their position respect to the rotor pole which is used in order to select the desired phase [5].
4. **Modulation Based Strategies**
   Position estimation in these strategies is based on the calculation of the phase inductance from the

modulated signal which obtains from the phase winding (includes: Frequency Modulation (FM) [6], Amplitude Modulation (AM) [7] and Phase Modulation (PM) [8]).

5. **Chopping Strategy**
   In this method, the variation of the active phase current in a period of time is used in rotor position estimation [9].
6. **Observer Based Strategy**
   In this technique, the SRM and its mathematical model which is designed in computer are run at the same time. The rotor position information obtained in the computer is used to drive the real SRM [10].
7. **Mutual Voltage Strategy**
   As the motor works, active phase induces some voltage to other inactive phases whose amplitude is used in rotor position detection in this method [11].
8. **Resonance Strategy**
   In resonance method, a low level pulse with specific frequency is applied to inactive phase. The pulse frequency is designed to create a resonance in the phase inductance in the unaligned position of the rotor [12].
9. **Series Capacitor Strategy**
   A capacitor is placed in series with the phase winding and low level pulses are applied to the phase. The charging time of the capacitor is utilized in rotor position estimation [13].
10. **Flux Calculation Strategy**
    By sampling the active phase current and calculating the flux, rotor position is able to be calculated [14].
11. **Current Waveform Strategy**
    At different positions of the rotor pole, the active phase current waveform differs which is utilized in rotor position estimation in this technique [15].
12. **Intelligent Control Strategy**
    In these strategies, Fourier series or intelligent controllers like fuzzy, neural networks, etc are implemented in rotor position estimation [16].

SRM is a special machine with salient rotor and stator poles which has many advantages like simplicity, low cost, high efficiency, ability to work in harsh environment, etc. The no-winding rotor poles make the motor to be able to reach higher speed than other types of motors. On the other hand, the motor cooling is much easier. The simplicity of SRM causes it to require less maintenance.There are two types of SRMs: Linear SRM (L-SRM) and the Rotary SRM (R-SRM). The L-SRM is divided into Single Stack (LSS) SRM and Multi Stack (LMS) SRM. The R-SRM has two types of Radial Field (RRF) SRM and Axial Field (RAF) SRM.

In some RRF-SRMs, the rotor is the outer part and the stator is the inner part. In some others, the rotor is rotated inside the stator. The RAF-SRM has two types of multi stack with internal rotor and single stack with external rotor. The general classification of SRMs is shown in Figure 2 [17-20].

In this paper, a low cost sensorless driver circuit is designed, constructed and tested on two types of three-phase SRMs. In the presented driver, a novel sensorless method is introduced in order to control SRM in low speed. The method uses simplified equation of the motor phase which is obtained from linear magnetization curve of the SRM. This novel technique decreases the control calculations, therefore, no expensive and high frequency controller chip is required and the written program is not complex as well. The controller circuit is also low cost and simple. (Note that, most of the usual sensorless techniques need computer or high frequency controller chip in order to drive the motor which are expensive components.)

Two other methods are also utilized to start the motor from standstill and control it in high speed. They are used in order to show the compatibility of the presented novel method with other usual methods. Note that, different methods are required in SRM control which depends on the amount of the motor speed.

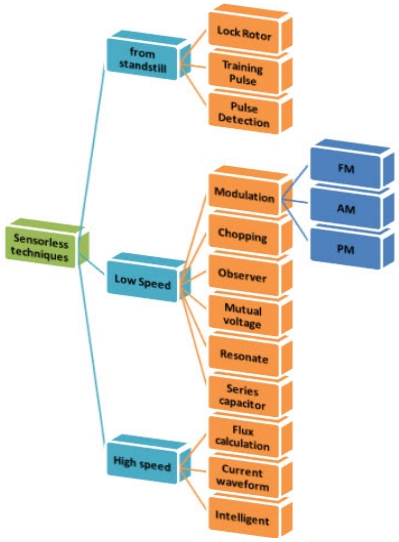

Figure 1. Sensorless techniques classification

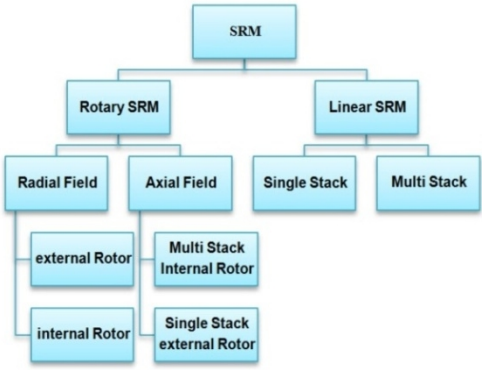

Figure 2. SRMs classification

According to the previous paragraph, the board operates in three steps and control algorithms. One of them is an open-loop technique which is used to start the motor. Second one uses linear magnetization curve of the motor in order to control the SRM in low speed. The last step uses current waveform of the active phase to detect the rotor position and control the motor in high speed. The motor parameters that are required in the control algorithm are obtained by analyzing the motor in software by FEM. The circuit is designed and used in order to drive two types of motors in laboratory. They are 6 by 4 and 12 by 8 three-phase RRF SRMs with internal rotor. The controller component is an Atmega128 AVR chip which is an inexpensive microcontroller. Asymmetric bridge converter is used in order to excite the winding of the SRM phases. The operational results and waveforms of the sensorless circuit and the SRMs which are obtained in the laboratory are compared as well.

This paper is organized as follows: Section II presents the specifications of the 6 by 4 and 12 by 8 three-phase SRMs. The SRMs are also simulated and analyzed by FEM in this section. In section III, the sensorless driver circuit, the novel and other control algorithms are designed. In section IV, the sensorless driver circuit is constructed and tested in laboratory by controlling the selected 6 by 4 and 12 by 8 SRMs. The operational results and waveforms are obtained and shown in figures then. The conclusions and the comparison of the results are presented in section V.

2. THE SPECIFICATIONS AND SIMULATION OF 6 BY 4 AND 12 BY 8 THREE-PHASE RRF SRMS

In this section, one 6 by 4 and one 12 by 8 three-phase RRF SRMs with internal rotor are selected and their specifications are explained. Then, they are analyzed by FEM in order to obtain their parameters.

2. 1. The Specifications of the SRMs Both of the presented SRMs are built in a same motor housing with a same volume. The 6 by 4 and 12 by 8 SRMs are shown in Figure 3 (a) and (b), respectively.

The rotor shape and windings of the selected SRMs are illustrated in Figure 4. In SRM designing, more poles means the motor has lower speed, higher torque level and also lower torque ripple.

The specifications of the presented 6 by 4 three-phase SRM are presented in Table 1. The rotor pole arc is 32° while the stator pole arc is 30°. The difference between the arc of the rotor and stator poles helps the motor to have lower torque ripple. The stator has the diameter of 60 mm and the rotor has the diameter of about 35 mm. There is 0.25 mm air gap between the rotor and stator poles. Each coil in this motor includes 200 turns winding. The motor has about 50 W power in 12 V supply voltage. The nominal speed of the motor is 5000 rpm.

(a)

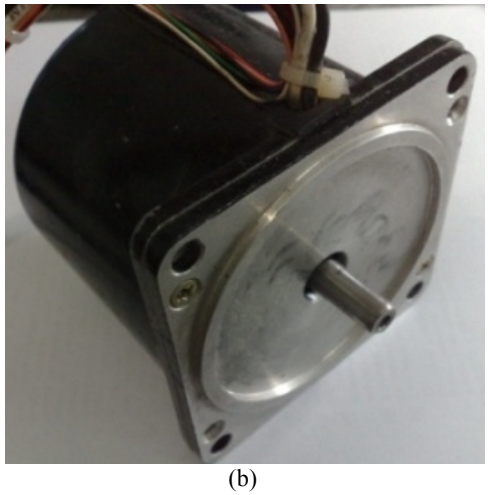

(b)

Figure 3. (a) 6 by 4 three-phase SRM and (b) 12 by 8 three-phase SRM

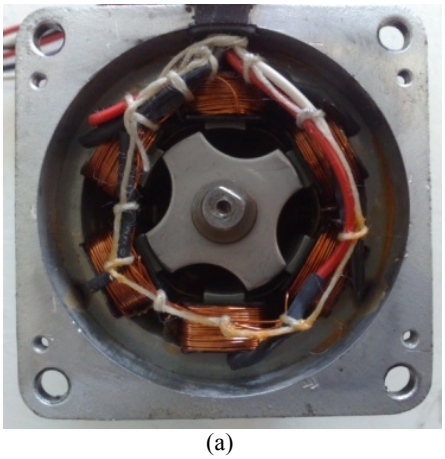

(a)

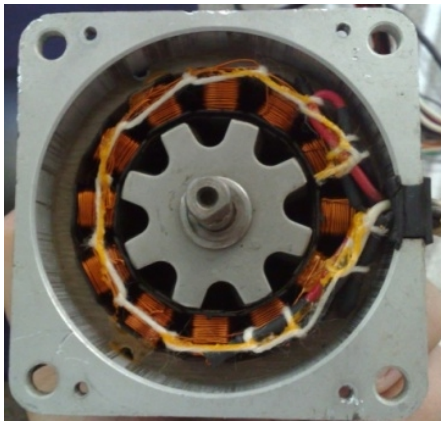

(b)

Figure 4. Rotor shape: (a) 6 by 4 three-phase SRM and (b) 12 by 8 three-phase SRM

TABLE 1. The specifications of the 6 by 4 three-phase SRM

Nominal power	50 W
Nominal voltage	12 V
Nominal speed	5000 rpm
Stator core outer diameter	60 mm
Stator core inner diameter	52 mm
Stator pole arc	30°
Air gap	0.25 mm
Rotor core outer diameter	35 mm
Rotor shaft diameter	8 mm
Rotor pole arc	32°
Number of turns per pole	200

TABLE 2. The specifications of the 12 by 8 three-phase SRM

Nominal power	50 W
Nominal voltage	12 V
Nominal speed	3000 rpm
Stator core outer diameter	60 mm
Stator core inner diameter	52 mm
Stator pole arc	14°
Air gap	0.25 mm
Rotor core outer diameter	35 mm
Rotor shaft diameter	8 mm
Rotor pole arc	16°
Number of turns per pole	150

The specifications of the introduced 12 by 8 three-phase SRM are presented in Table 2. The rotor pole arc is 16° while the stator pole arc is 14°. The stator has the diameter of 60 mm and the rotor has the diameter of about 35 mm. There is 0.25 mm air gap between the rotor and stator poles. Each coil in this motor includes 150 turns winding. The motor has about 50 W power in 12 V supply voltage. The nominal speed is about 3000 rpm in this SRM.

Both of the presented 6 by 4 and 12 by 8 SRMs are three-phase but the 12 by 8 SRM has lower speed than the 6 by 4 SRM because it has more poles. It is able to generate higher torque level with lower torque ripple rather than the 6 by 4 SRM.

2. 2. The Simulation of the SRMs The parameters of the SRMs can be obtained in simulation. Magnet CAD package which uses FEM numerical technique is implemented in order to find solution for partial differential and integral equations. Two common methods are implemented to solve magnetic field problems. One of them uses electric vector potential and the other uses magnetic vector potential. In Magnet CAD package in which electric vector potential is used, the final two scalar equations are [21]:

$$\nabla^2 T - \mu\sigma\left(\frac{\partial T}{\partial t}\right) = -\mu\sigma\nabla\left(\frac{\partial \Omega}{\partial t}\right) \quad (1)$$

$$\nabla^2 \Omega = 0 \quad (2)$$

The SRMs are simulated in Magnet software by FEM. In Magnet, different rotor positions are defined as some problems. After that, the phase winding is excited by DC current and the rotor is rotated in the desired direction. Then, Magnet obtains the SRM parameters for each problem.

In this paper, the phase winding in each selected SRM is excited by 0.1A to 3A rated current and every time, the motor is simulated and the rotor is rotated from the beginning of alignment to fully aligned position and then to unaligned position.

In Figure 5, the flux density and flux path are shown in the 12 by 8 three-phase SRM for different positions of the rotor and 3A rated current of the phase. As it is shown, four poles are excited as a phase in this motor. Figure 5(a) illustrates the flux density and flux path at the beginning of alignment position of the rotor. The maximum value of flux density is about 1.141 Tesla in this position. Figure 5 (b) is for half aligned position of the rotor where the flux density is about 1.394 Tesla. Figure 5 (c) is for fully aligned position of the rotor and the maximum value of flux density is about 1.397 Tesla there.

Figure 6 depicts the flux density and flux path of the selected 6 by 4 three-phase SRM in different positions of the rotor and 3A rated current of the phase winding. As it is illustrated, two poles are excited as a phase in this SRM. The flux begins to move from the stator tooth, moves from air gap, the rotor and the other stator

tooth and then closes its path from the yoke. Figure 6 (a) shows the flux density and flux path at the beginning of alignment position where the maximum value of flux density is about 0.96 Tesla. Figure 6 (b) belongs to half aligned position of the rotor. The maximum value of flux density is about 0.99 Tesla there. In Figure 6(c), which shows the fully aligned position of the rotor, the maximum value of flux density is about 1.06 Tesla.

A large number of SRM parameters are obtained in Magnet software by using FEM e.g. flux, torque, torque ripple, windings energy, losses .etc but the information related to flux are more important in designing of the presented sensorless circuit. In fact, in the design, the relation existing between the flux, current and rotor position (which is named magnetization curve) is needed. The magnetization curves of the selected SRMs are also obtained by Magnet software after FEM analysis.

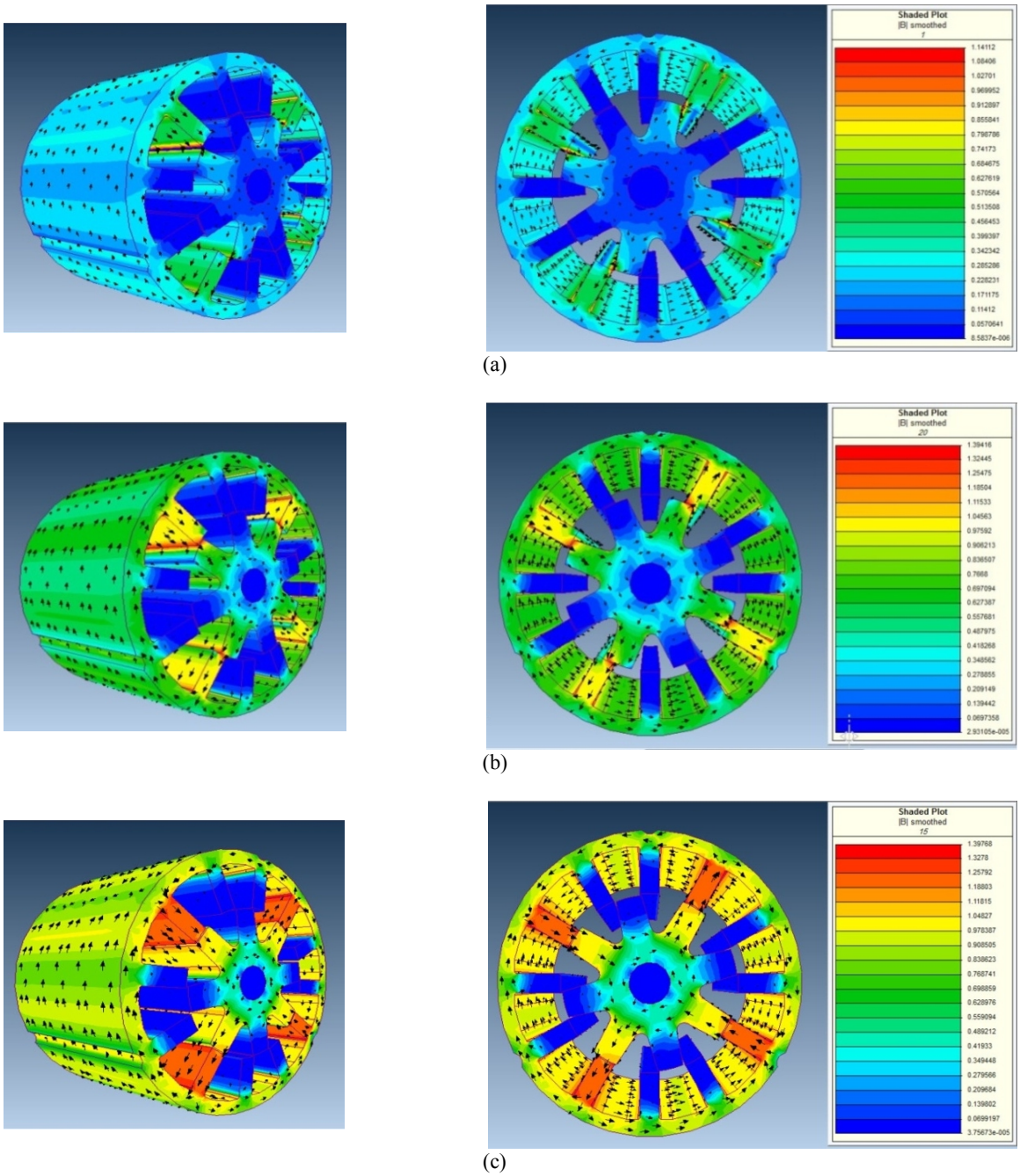

(a)

(b)

(c)

Figure 5. Flux density and flux path in the selected 12 by 8 SRM for: (a) beginning of alignment position, (b) half aligned position and (c) Fully aligned position

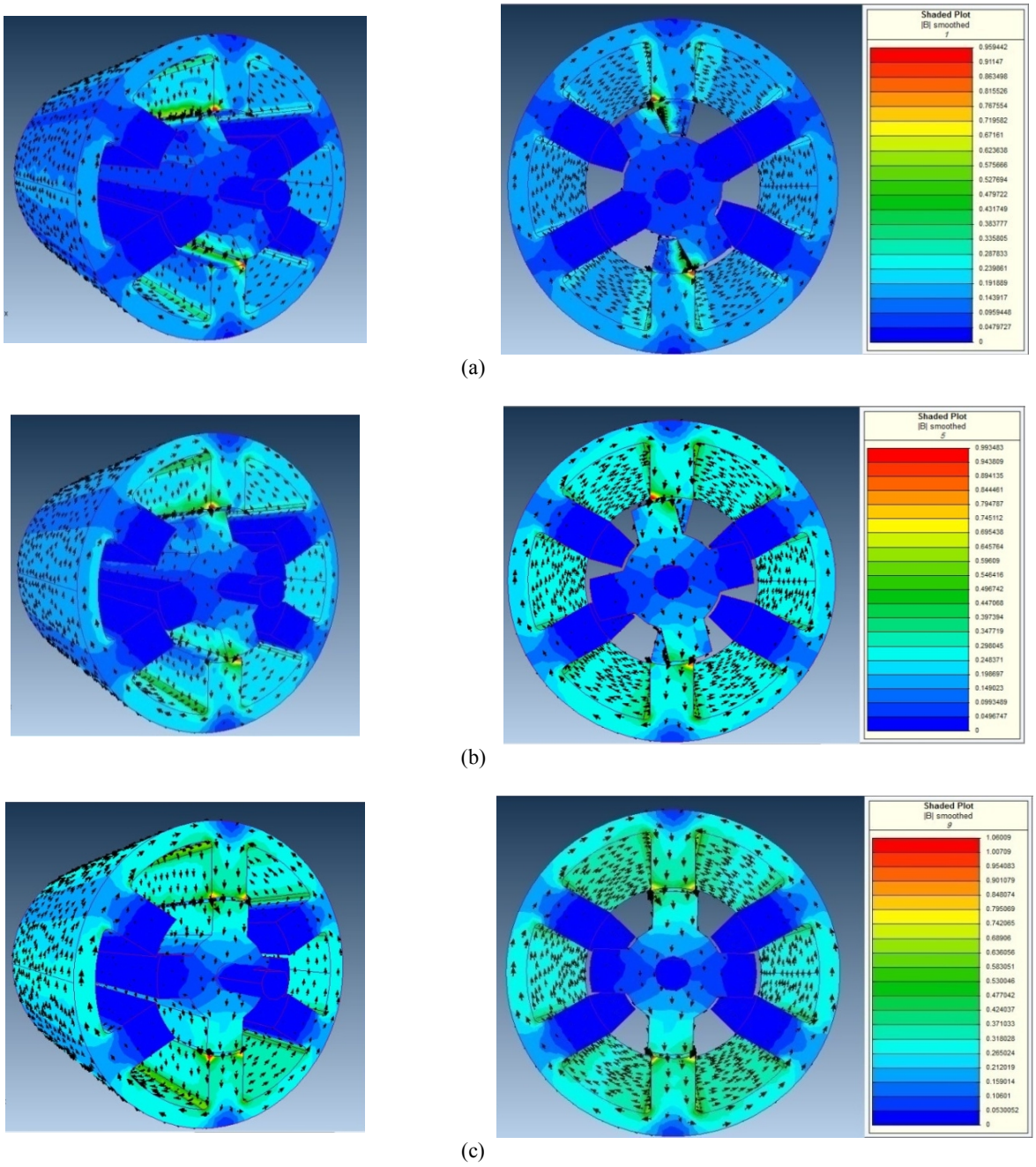

(a)

(b)

(c)

Figure 6. Flux density and flux path in the selected 6 by 4 SRM for: (a) beginning of alignment position, (b) half aligned position and (c) fully aligned position

Figure 7 shows the magnetization curve of the selected 12 by 8 three-phase SRM for the phase current of 0.1A to 3A and different rotor positions which is obtained in Magnet software. At the beginning of alignment position, the flux has its minimum value and in fully aligned position, the flux has its maximum value. In a specified position of the rotor, if the current of the phase winding increases, the flux will increase as well. This is explained in the section III completely.

Figure 8 illustrates the magnetization curve of the selected 6 by 4 three-phase SRM for the phase rated current of 0.1A to 3A and different positions of the rotor that is resulted in Magnet software.

Table 3 is a comparative table which shows some parameters of the SRMs obtained in Magnet.

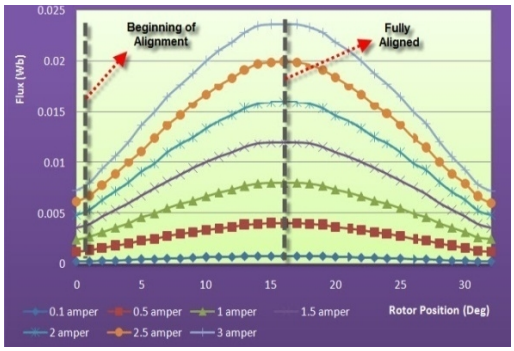

Figure 7. Magnetization curve of the 12 by 8 SRM

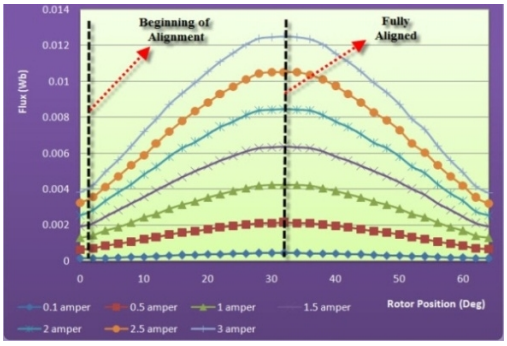

Figure 8. Magnetization curve of the 6 by 4 SRM

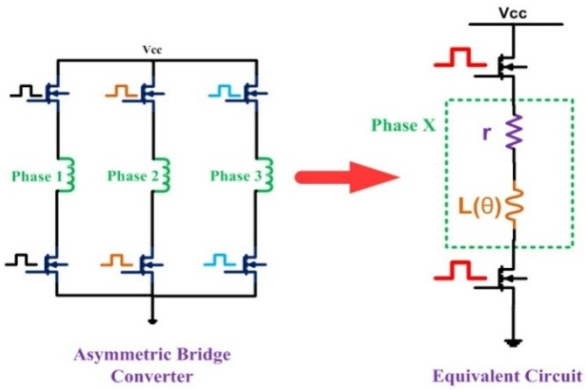

Figure 9. Equivalent circuit of SRM stator phase

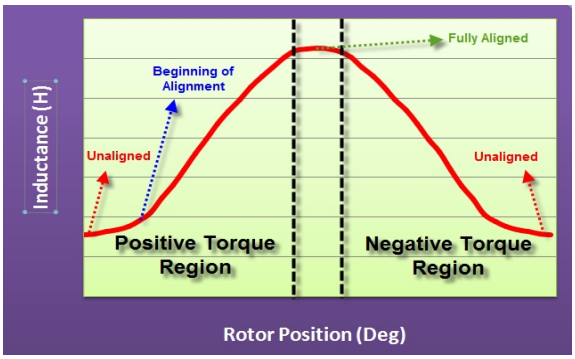

Figure 10. Phase inductance versus rotor position

TABLE 3. Some parameters obtained in Magnet for the 12 by 8 and 6 by 4 three-phase SRMs

Parameters obtained in Magnet	Unit	6/4	12/8
Flux density (MAX)	Tesla	1.06	1.397
Flux linkage (MAX) in 3 Ampere	Wb	0.013	0.024
Flux linkage (MIN) in 0.1 Ampere	Wb	0.000128	0.000242
Inductance (MAX)	H	31.5	51.4
Inductance (MIN)	H	5.1	10.3

3. THE NOVEL IDEA AND SENSORLESS DRIVER DESIGNING

In order to design the sensorless driver circuit, the basic relations of SRM, magnetization curve and motor parameters are required. In the presented sensorless driver, the motor is controlled in three steps. At first, the motor is started from standstill by training pulse method. In low speed, it is controlled by the linear magnetization curve. In high speed, it is controlled by current waveform technique.

The usual converter to drive and excite the SRM phase is an asymmetric bridge (two switches per phase) converter. Figure 9 illustrates an asymmetric bridge converter which is able to drive a three-phase SRM. As it is shown, the stator phase winding of the motor has an RL equivalent circuit, where r is the phase winding resistance in Ohm. θ is the rotor position. $L(\theta)$ is the winding inductance in Henry which depends on θ. In fact, $L(\theta)$ has different values in any position of the rotor which is shown in Figure 10. In unaligned position where a large air gap exists between the stator and rotor poles, the phase reluctance (R) value is high. According to the equation $L=N^2/R$, higher reluctance means lower inductance; as a result, in unaligned position, the inductance has its minimum value. On the contrary, in fully aligned position where the smallest air gap exists between the stator and rotor poles, the value of reluctance and inductance are minimum and maximum, respectively. Note that, the positive torque region is used in motor mode and negative torque region is used in generator mode of SR machines.

As it was explained, the stator phase winding of the motor has an RL equivalent circuit, so Equation (3) can be written for the equivalent circuit:

$$V = \frac{d\lambda(\theta,i)}{dt} + ri \quad (3)$$

where V is the phase voltage in Volt, i is the phase current in Ampere, θ is the rotor position angle in Radian, $\lambda(\theta,i)$ which depends on i and θ is flux linkage in Weber.

Using partial derivative, the general and basic SRM equation is obtained [22]:

$$V = ri + \frac{\partial \lambda}{\partial i}\frac{di}{dt} + \omega\frac{\partial \lambda}{\partial \theta} \quad (4)$$

where $\omega = \frac{d\theta}{dt}$ is the angle speed of the rotor in rad/sec. Equation (4) is the basic equation for a large number of sensorless control methods to detect rotor position. In SRM control, the rotor position is the most important parameter which has to be obtained. The winding current, flux linkage, applied voltage, resistance and also the speed of the rotor are needed for calculating the rotor position in the presented sensorless control system. The rotor speed can be easily calculated by the controller from the phase switching frequency. The phase applied voltage is known. The winding current is sampled by the controller. The value of the winding resistance is measured by multimeter and is a constant value in the equation.

Generally, the magnetization curve (λ-θ-i) is saved as a three-dimensional Look up Table (LUT) in the controller memory in order to calculate and detect the rotor position. The LUT information has to be calculated by additional software for different values of these parameters. Sometimes the SRM equations are placed in the controller programs and each time the rotor position is calculated from the sampled phase current using these equations. So the estimation of rotor position is somehow complex and requires robust and high speed controller with a large memory and of course high price like Digital Signal Processor (DSP).

The SRM phase should be switched on near to beginning of alignment region and switched off near to fully aligned region. By looking at the magnetization curves (Figures 7 and 8) deeply, it is realized that the magnetization curve can be assumed to be linear in the region between the beginning of alignment and fully aligned points for each value of current. The linear magnetization curves of the selected 12 by 8 and 6 by 4 SRMs are presented in Figure 11(a) and (b), respectively. More studies show that the λ-i curve can also be assumed to be linear between these points as it is illustrated in Figure 12. Using this novel idea, only two simple linear equations for λ-i curve and λ-θ curve are saved in the controller memory and used to estimate the rotor position by Equation (4). This decreases the calculations; as a result, a low cost controller chip with usual frequency is able to drive the motor. In fact, in the novel method, the current of the active phase is sampled and then the flux is calculated. Using this information, the rotor position is detected. But this detection is implemented much easier and quicker than usual similar methods. As an example, for the selected 12 by 8 three-phase SRM, the λ-θ equation is obtained as Equation (5) for one sampled phase current:

$$\lambda = 0.1627\lambda_{14}.\theta - 1.278\lambda_{14} \quad (5)$$

where λ_{14} is the value of flux in rotor position of 14° (beginning of alignment position) and calculated from λ-i equation:

$$\lambda_{14} = \frac{i}{100} \times \lambda_0 \quad (6)$$

where i is the sampled phase current and λ_0 is the flux in rotor position of 14° for 100 mA phase current and equal to 241×10^{-6} Wb for the selected 12 by 8 SRM. Equation (6) is obtained from Figure 12 which shows that the λ-i curve is also linear. Using these equations and Equation (4), $\frac{\partial \lambda}{\partial i} = L(\theta)$ is calculated and from Equation (5), θ is calculated for the sampled current. After detection of the rotor position, the adequate command pulses are produced in order to control the motor.

(a)

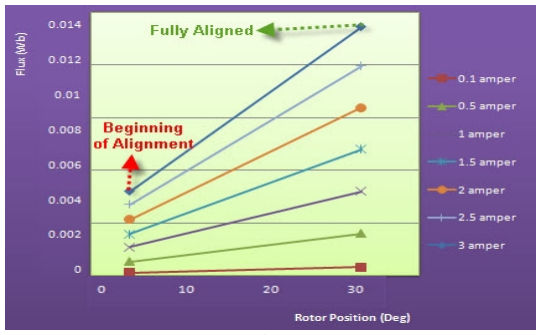

(b)

Figure 11. Linear magnetization curves of the selected SRMs: (a) 12 by 8 and (b) 6 by 4

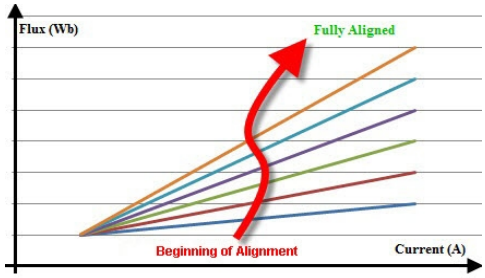

Figure 12. SRM λ -i curve

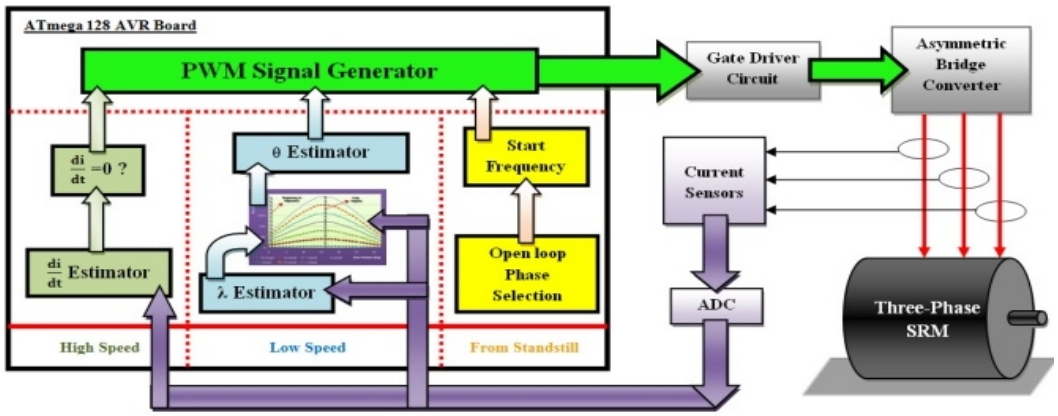

Figure 13. Block diagram of the constructed sensorless driver circuit

4. CONSTRUCTION OF THE SENSORLESS DRIVER CIRCUIT

The block diagram of the constructed three-phase sensorless driver circuit is illustrated in Figure 13. The board has a 12 V DC power supply and uses Lm7805 voltage regulator to generate 5 V in order to use for microcontroller and other digital chips. The controller is an Atmega128 AVR microcontroller board. It operates with 16 MHz clock frequency. As it is shown, there are three control algorithms in the microcontroller board: 1- starting motor from standstill, 2- controlling in low speed and 3- controlling in high speed.

According to these algorithms, the desired pulses are generated to control the SRM using Pulse Width Modulation (PWM) technique in PWM signal generator. In fact, the PWM signal generator section generates the gate pulse of transistors used in converter. The SRM phase excitation is done by an asymmetric bridge converter in the presented paper by two IRF540 N-channel Mosfets in each phase. Mosfets need Mosfet driver. HIP2500 Mosfet driver is used in the gate driver circuit for each phase to drive the Mosfets. In the shown asymmetric bridge converter, each phase of the motor is excited respectively which causes the motor rotates in the desired speed and direction.

As it is illustrated in the block diagram, step 2 (low speed) and step 3 (high speed) of the control algorithm require the value of the phase current to drive the motor. The current of each phase is sampled by 1 MHz frequency by an ASC712 which is a Hall effect-based linear current sensor. The output of the current sensor is a low amplitude analogue signal which is converted to digital data by a power full 10 bit Analogue to Digital Converter (ADC). These digital data are then transmitted to the controller board. The three steps of the control algorithm are done as follows:

In standstill, training pulse method which is an open-loop technique is used to generate commands to start the motor. One of the phases of the SRM is selected and trains of pulse are applied to the phase. This is done for other phases frequently with a desired start frequency according to the desired starting speed. The generated commands are then transferred to PWM signal generator section in order to generate gate pulses of the transistors.

In low speed, the linear magnetization curve of the motor is used to estimate the rotor position. The general algorithm which is used to control the SRM in low speed is shown in Figure 14. As it is shown, one phase of the SRM is excited (N=1) at first. After that, the phase current is sampled by the current sensor which is given to the control board after converting to digital data. Then the flux is calculated by Equation (3).

In the next step, the value of the rotor position is obtained using the linear magnetization curve, value of flux and phase current. If the rotor is in fully aligned position ($\theta_{desired}$), the phase is turned off and the next phase is excited (N=N+1); otherwise, the processes continue till the desired rotor position. The presented SRMs have three phases so after exciting the third phase, the first phase is excited again (N=1). This algorithm is repeated in low speed.

In high speed, current waveform technique is implemented to detect the rotor position. The current of the active phase is sampled by the current sensor and converted to digital data by the ADC. When the slope of the current waveform is zero, the rotor is at the beginning of alignment position which means the phase should be excited. This property is basically because of the inductance value of the phase winding. In fact, in unaligned position, the value of the phase inductance is low which causes the phase current to increase very quickly after phase excitation (the slope of the current waveform is positive). At the beginning of alignment

position, the phase inductance starts to increase immediately which prevents the phase current to increase. In this position, the value of the phase current is constant for a moment (the slope of the current waveform is zero). After that, the phase inductance increases which causes the phase current to decrease (the slope of the current waveform is negative).

4. 1. Three-Phase 6 by 4 SRM Driving and Operational Results The constructed circuit is first adjusted and programmed for the 6 by 4 three-phase SRM in laboratory. Note that, the SRMs are driven in no-load condition in the presented paper. At the first step, the motor starts rotation from standstill by training pulse method. The operational results are shown for two phases of the motor in Figure 15. Figure 15(a) shows the PWM output signal of the AVR board which is then amplified by the HIP2500 Mosfet driver and connected to the gate of the transistors. The drain voltage of the Mosfet is illustrated in Figure 15(b). Figure 15(c) depicts the output waveform of the ASC712 current sensor. As it is shown in figures, in PWM signal generating the pervious phase is not turned off immediately after excitation of the next phase which reduces the noise and torque ripple in the SRM. In fact, the next phase is turned-on before the previous phase is turned-off. This helps the motor to generate torque with less torque ripple.

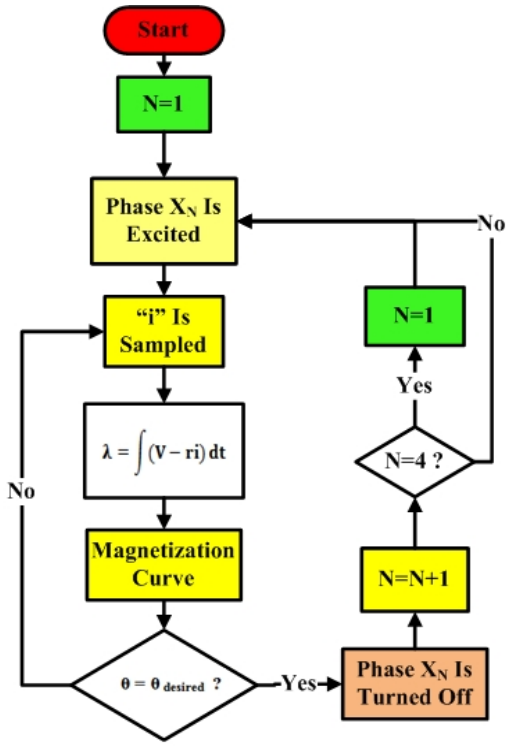

Figure 14. The general control algorithm using linear magnetization curve in low speed

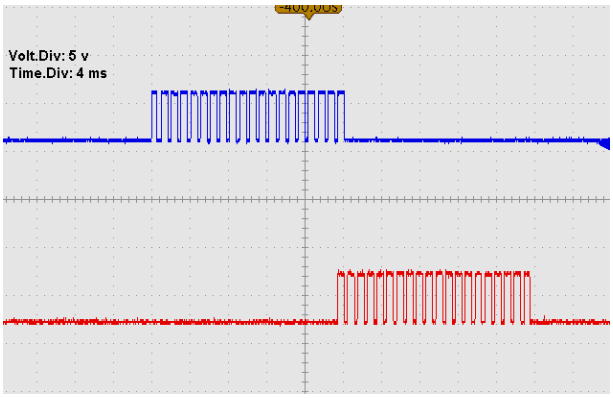

(a)

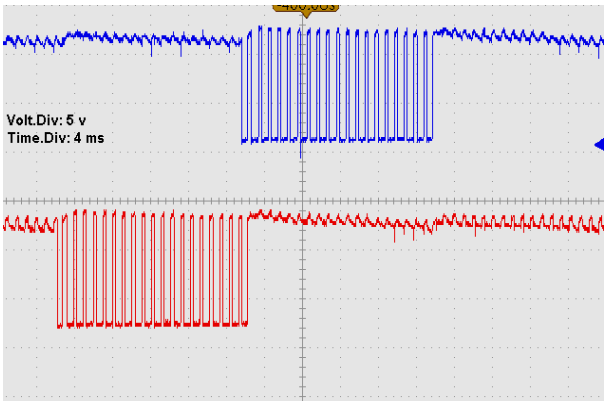

(b)

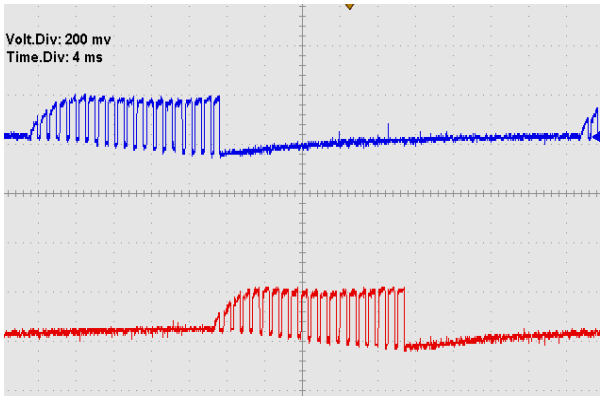

(c)

Figure 15. Starting from standstill in 6 by 4 SRM: (a) PWM output signal of the microcontroller board, (b) drain voltage of the upper transistor and (c) output voltage of ASC712 current sensor

After reaching to 400 rpm speed, the board changes the control algorithm and uses the linear magnetization curve algorithm. By increasing the switching frequency the speed of the SRM increases. The linear magnetization curve algorithm is used from the speed of 400 rpm up to 2000 rpm for the selected 6 by 4 SRM. The operational results are shown in Figure 16 for the

speed of about 800 rpm of the 6 by 4 SRM. As it is shown, in this step, chopped pulses are used which means we are able to have any under-load control algorithms (torque or speed control) by changing the duty cycle of the pulses. After 2000 rpm speed, the controller enters the third step of the control algorithm which is a single pulse algorithm using current waveform technique. This step is implemented from the speed of about 2000 rpm up to nominal speed (about 5000 rpm). The operational results are shown in Figure 17 for the speed of about 4500 rpm for the 6 by 4 SRM. The Gate-Source and Drain-Source voltage of the lower Mosfet in one phase of the asymmetric bridge converter are shown in Figure 17(a). The same waveforms are depicted in Figure 17(b) for the upper Mosfet. Figure 17(c) shows the output waveform of the ASC712 current sensor for two phases.

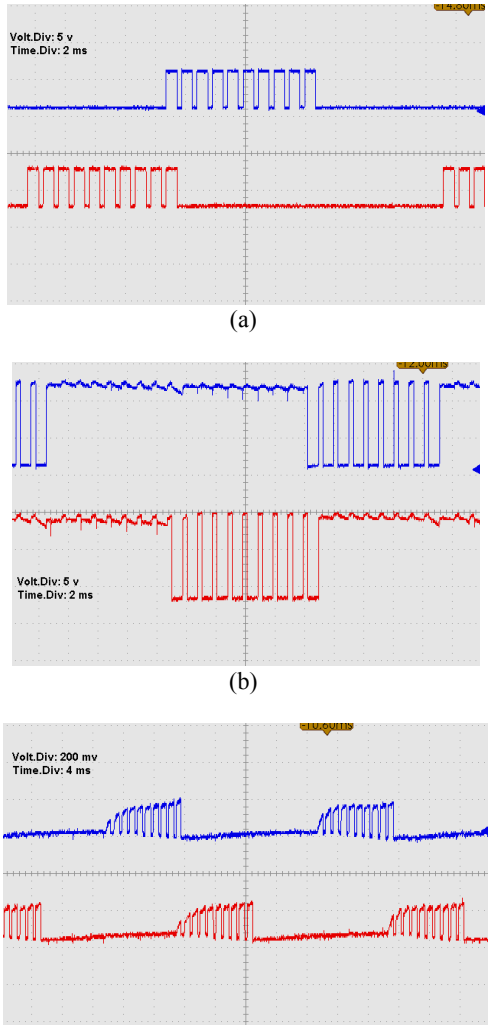

Figure 16. Operating in 800 rpm speed in 6 by 4 SRM: (a) PWM output signal of the microcontroller board, (b) drain voltage of the upper transistor and (c) output voltage of ASC712 current sensor

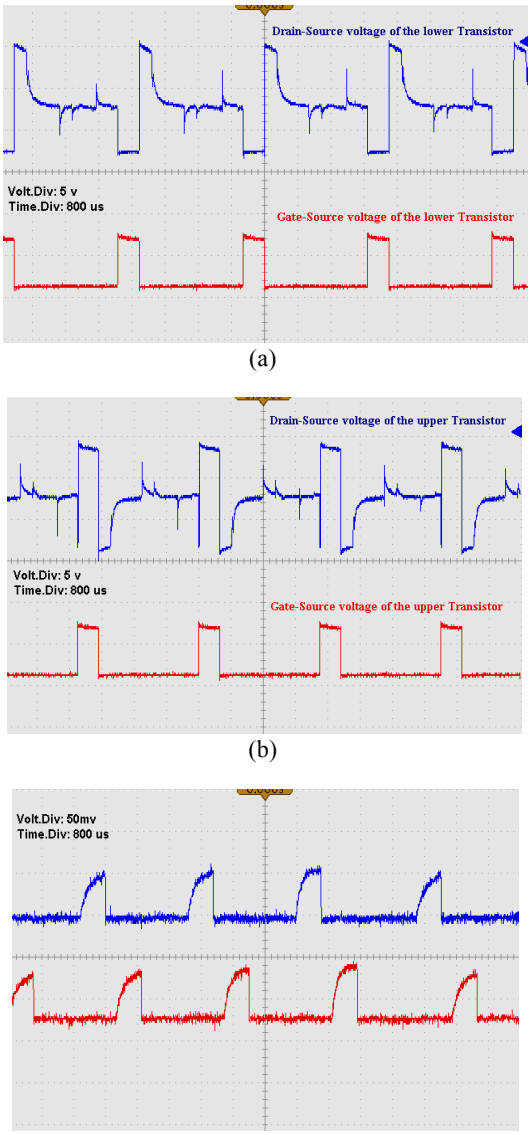

Figure 17. Operating in 4500 rpm speed in 6 by 4 SRM: (a) Gate-Source and Drain-Source voltage of the lower transistor, (b) Gate-Source and Drain-Source voltage of the upper transistor and (c) output voltage of ASC712 current sensor

4. 2. Three-Phase 12 by 8 SRM Driving and Operational Results The constructed sensorless driver circuit is then programmed for the presented 12 by 8 three-phase SRM. Again, at the first step, the SRM starts rotation from standstill by the training pulse technique. Figure 18 illustrates the laboratory results of this step. Figure 18(a) depicts the PWM output signal of the AVR board for two phases of the SRM. The drain voltage of transistor is shown in Figure 18(b). Figure 18(c) presents the output waveform of the ASC712 current sensor.

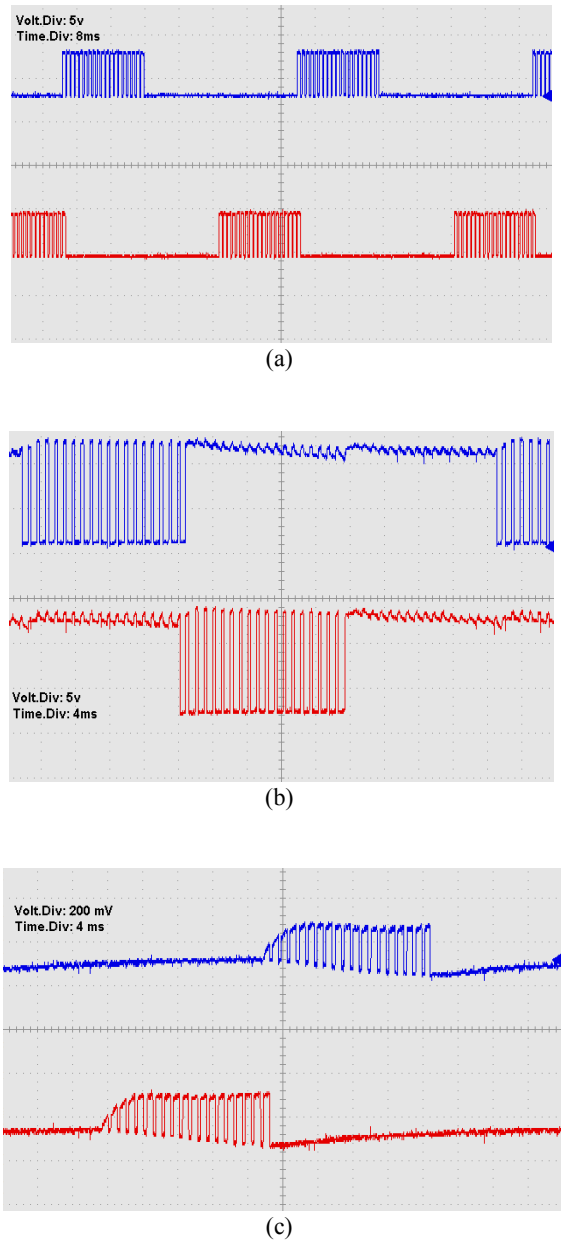

Figure 18. Starting from standstill in 12 by 8 SRM: (a) PWM output signal of the microcontroller board, (b) drain voltage of the upper transistor and (c) output voltage of ASC712 current sensor

At the speed of about 400 rpm, the sensorless board changes the control algorithm to the linear magnetization curve algorithm. For the presented 12 by 8 three-phase SRM, the linear magnetization curve algorithm can be used from the speed of about 400 rpm up to 1800 rpm. The operational results at the speed of about 1050 rpm are shown in Figure 19.

At 1800 rpm speed, the controller enters to the next control algorithm which is the current waveform method. This algorithm is used from the speed of about 1800 rpm up to nominal speed of the selected 12 by 8 SRM (about 3000 rpm). The operational results are illustrated in Figure 20 for the speed of about 2200 rpm.

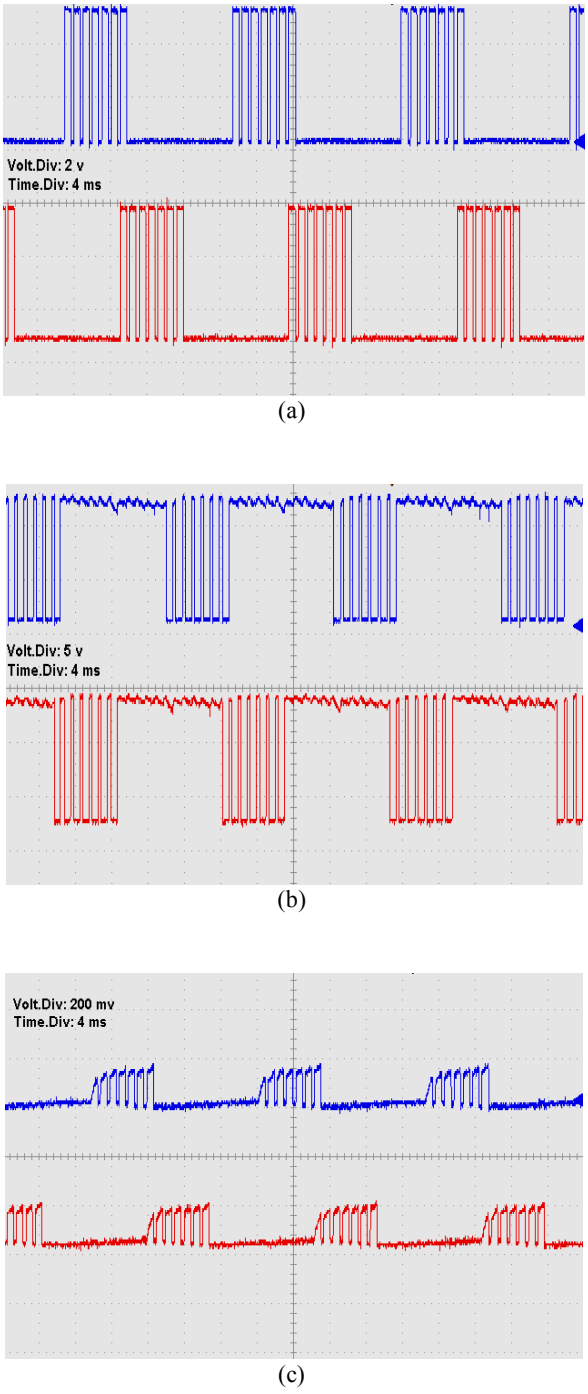

Figure 19. Operating in 1050 rpm speed in 12 by 8 SRM: (a) PWM output signal of the microcontroller board, (b) drain voltage of the upper transistor and (c) output voltage of ASC712 current sensor

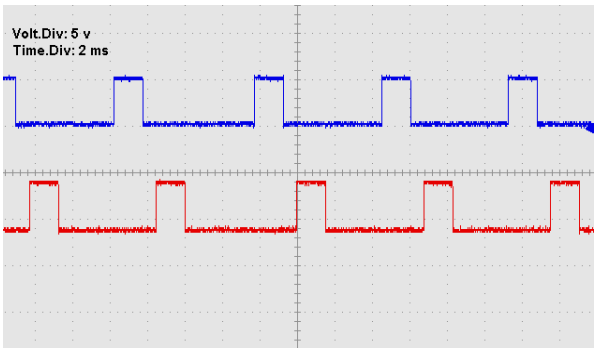

(a)

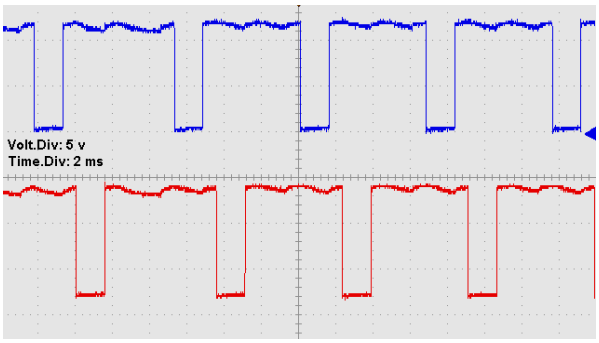

(b)

(c)

Figure 20. Operating in 2200 rpm speed in 12 by 8 SRM: (a) PWM output signal of the microcontroller board, (b) drain voltage of the upper transistor and (c) output voltage of ASC712 current sensor

5. CONCLUSION

This paper presented the design, construction and testing of a sensorless driver circuit for one 12 by 8 and one 6 by 4 three-phase RRF SRMs with internal rotor. The driver circuit used three control algorithms for three ranges of operational speed which were: training pulse technique (from standstill), linear magnetization curve method (in low speed) and current waveform technique (in high speed). Each sensorless control technique was proper for specified range of speed. The linear magnetization curve method was a novel sensorless technique introduced in this paper. This technique decreased the control calculations so inexpensive and usual controller component was required in order to control the SRMs. As a result, the sensorless board was simple and low cost. An inexpensive Atmega128 AVR chip was used as the controller component in the circuit. Asymmetric bridge converter with IRF540 N-channel Mosfets and HIP2500 Mosfet driver was used to excite the phase winding of the SRMs. The board was adjusted for each selected SRM and tested in laboratory. Then, the operational results and waveforms were shown.

The 12 by 8 three-phase SRM could reach to speed of about 3000 rpm by the presented circuit. After starting from standstill in step one, the SRM was controlled by the novel linear magnetization curve algorithm from the speed of 400 rpm up to 1800 rpm. Then, it was controlled by the current wave form control algorithm up to 3000 rpm speed.

The 6 by 4 three-phase SRM could reach to speed of about 5000 rpm by the presented circuit. The motor started rotation from standstill in the first step and then was controlled from the speed of about 400 rpm up to 2000 rpm by the second algorithm. In the last step, it was controlled by the third control algorithm up to 5000 rpm speed.

The 12 by 8 three-phase SRM could reach to speed of about 3000 rpm while the 6 by 4 three-phase SRM could reach to speed of about 5000 rpm because it had fewer poles than the 12 by 8 SRM. Generally, more poles means the motor has lower speed, higher torque level and also lower torque ripple.

6. REFERENCES

1. E. Afjei, O. Hashemipour, M. A. Saati and M. M. Nezamabadi, "A new hybrid brushless dc motor/generator without permanent magnet," ***International Journal of Engineering (IJE)***, Vol. 20, No. 1, (2007), 77-86.
2. E. Afjei, M. Fallah "An efficient drive circuit for switched reluctance motor," ***International Journal of Engineering (IJE)***, Vol. 12, No. 3, (1999), 137-143.
3. J.P. Lyons, and S.R. MacMinn, "Lock Detector For Switched Reluctance Machine Rotor Position Estimator," US Patent No. 5140244, (1992).
4. O.Ahmed, K. Ohyama, Y. Narumoto, H. Fujii and H. Uehara, "Sensorless Operation Of Srm Drives From Starting To Steady State," ***IEEE International Symposium on Industrial Electronics. Electron,*** (2002), 1269-1274.
5. E. Kayikci and R.D. Lorenz, "Self-Sensing Control of a Four Phase Switched Reluctance Drive Using High Frequency Signal Injection including Saturation Effects," ***IEEE Ind,*** (2009), 611-618.
6. M.Ehsani, I.Hosein and A.B.Kulkarani, "Elimination of Discrete Position Sensor and Current Sensor in Switched Reluctance Motor Drives," ***IEEE Trans on Power Electronics***, Vol. 28, No. 1, (1992), 128 - 135.
7. A.Moraveji, A. Siadatan, E. Afjei, M. Rafiee and E. Zarei Ali Abadi, "DSP Sensorless Controller of Switched Reluctance Motor-Generator Approaching to AM Modulation," ***IEEE Ind***, (2011), 1-5.

8. A.Najafi, E. Afjei and H. Khalili, "Rotor Position Detection in SRM Drive Utilizing Phase Shift Variations in a Formed Resonant Circuit," ***IEEE Ind,*** (2007), 1-5.
9. P.P. Acarnley, "Stepping Motors: A Guide to Modern Theory and Practice," ***Peter Peregrinus Ltd***, (1982).
10. L. Yu-zhou and Z. Ke-gang, "Sensorless Speed Control of the Switched Reluctance Motor Using Extended Kalman Filter," ***IEEE Ind,*** (2010), 1-4.
11. I.Hosein and M.Ehsani, "Rotor Position Sensing In Switched Reluctance Motor Drivers By Measuring Mutually Induced Voltages," ***IEEE Trans Ind.App,*** Vol. 30, No. 3, (1994), 665-672.
12. E. Afjei, "A New Resonant Convertor Circuit for Reluctance Motor," ***International Journal of Engineering (IJE)***, Vol. 12, (1999), 69-80.
13. E. Afjei, H. Moradi Cheshmeh Baygi, and H. Nouri, "Detecting the Rotor Position by Employing Pulse Injection Technique And Digital Pulse Width Modulation Decoder in Switched Reluctance Motor," ***IEEE Ind,*** (2010), 44-47.
14. Z. Yi-feng, G. Qiong-Xuan and C. Hao, "A New Position Sensorless Control Technology for Switched Reluctance Motor," ***IEEE Ind,*** (2010), 1-4.
15. W. Zeng, C. Liu, Q. Zhou, J. Cai and L. Zhang, "A New Flux/Current Method for SRM Rotor Position Estimation," ***IEEE Ind***, (2009). 1-6.
16. Qiuli LIU, et al, "Design of Electric Drive System with SRM and its Fuzzy Controller for Armored Vehicles," ***IEEE Ind***, (2011), 1187-1190.
17. Torkaman, H. and Afjei, E., "Comprehensive Magnetic Field based study on Effects of Static Rotor Eccentricity in Switched Reluctance Motor Parameters Utilizing three Dimensional Finite Element", ***Electromagnetics Journal, Taylor and Francis***, Vol. 29, (2009), 421-433.
18. Torkaman, H. and Afjei, E., "Comprehensive Study of 2-D and 3-D Finite Element Analysis of a Switched Reluctance Motor", ***Journal of Applied Science***, Vol. 8, No. 15, (2008), 2758-2763.
19. Cheewoo Lee, R. Krishnan, and N. S. Lobo, " New Designs of a Two-Phase E-Core Switched Reluctance Machine by Optimizing the Magnetic Structure for a Specific Application: Concept, Design, and Analysis ", ***IEEE. Industry Applications Society Annual Meeting,*** (2008), 1 – 8.
20. Wayne Pengov , J.R. Hendershot Jr , TJE Miller, "A new low-noise two-phase switched reluctance motor", *IEEE* ***International Conference Electric Machines and Drives***, (2005), 1281-1284.
21. Magnet CAD Package: User Manual, ***Infolytica Corporation Ltd***, Montreal, Canada. (2006)
22. R.Krishnan, "Switched Reluctance Motor Drivers: Modeling, Simulation, Analysis, Design and Application," *CRC Press*, (2001). .

Design, Construction and Comparison of a Sensorless Driver Circuit for Switched Reluctance Motor

M. Rafiee[a], E. Afjei[b] , A. Siadatan[a]

[a] *Department of Electrical Engineering, West Tehran Branch, Islamic Azad University, Tehran, Iran.*
[b] *Department of Electrical Engineering, Faculty of Electrical and Computer Engineering, Shahid Beheshti University, Tehran, Iran*

PAPER INFO

Paper history:
Received 27 March 2013
Received in revised form 27 April 2013
Accepted 20 June 2013

Keywords:
Sensorless
SRM
FEM

چکیده

در مقاله ارائه شده، یک مدار راه انداز بدون سنسور برای کنترل دو نوع موتور رلوکتانس سوییچی سه فاز طراحی، ساخته و تست می گردد. الگوریتم کنترلی ارائه شده شامل سه مرحله است. در مرحله اول، موتور رلوکتانس سوییچی با یک روش حلقه باز راه اندازی و کنترل می شود. در مرحله دوم، یک روش جدید معرفی می شود که در آن از رابطه شار-جریان- موقعیت روتور بهینه شده، به منظور محاسبه موقعیت روتور و پس از آن کنترل موتور در سرعت پایین استفاده می گردد. در مرحله سوم، از شکل موج جریان فاز تحریک شده به منظور کشف موقعیت روتور و کنترل موتور در سرعت بالا استفاده می شود. به دلیل استفاده از روش جدید ارائه شده، یک مدار راه انداز بدون سنسور ساده و ارزان قیمت طراحی شده است. در این مدار ، از یک میکروکنترلر ارزان قیمت Atmega128 از خانواده AVR برای پیاده سازی الگوریتم های کنترلی و تولید پالس گیتهای ترانزیستورها استفاده شده است. از کانورتر پل دو سوییچه با ماسفتهای نوع N به منظور تحریک سیم پیچ فازها استفاده شده است. پارامترهایی از موتورهای رلوکتانس سوییچی که برای طراحی مدار راه انداز بدون سنسور احتیاج است، از طریق شبیه سازی و تحلیل موتورها توسط روش اجزا محدود بدست آمده اند. مدار ساخته شده در آزمایشگاه توسط موتورهای انتخاب شده در شرایط بی باری تست می شود و نتایج عملی بدست آمده و درآخر با یکدیگر مقایسه می گردند.

doi: *10.5829/idosi.ije.2014.27.01a.17*.